https://doi.org/10.5194/amt-2020-45
Preprint. Discussion started: 25 March 2020

Atmospheric Measurement Techniques Discussions

Simultaneous leaf-level measurement of trace gas emissions and photosynthesis with a portable photosynthesis system

Mj Riches, Daniel Lee, Delphine K. Farmer

Department of Chemistry, Colorado State University, Fort Collins, 80523, USA

Correspondence to: Delphine K. Farmer (Delphine.Farmer@colostate.edu)

Abstract. Plants emit considerable quantities of volatile organic compounds (VOCs), the identity and amount of which vary with temperature, light and other environmental factors. Portable photosynthesis systems are a useful method for simultaneously quantifying in situ leaf-level emissions of VOCs and plant physiology. We present a comprehensive characterization of the LI-6800 portable photosynthesis system's ability to be coupled to trace gas detectors and measure leaf-level trace gas emissions, including limits in flow rates, environmental parameters, and VOC backgrounds. Instrument contaminants from the LI-6800 can be substantial, but are dominantly complex molecules such as siloxanes that are structurally dissimilar to biogenic VOCs and thus unlikely to interfere with most leaf-level emissions measurements. We validate the method by comparing CO_2 assimilation calculated internally by the portable photosynthesis system to measurements taken with an external CO_2 gas analyzer; these assimilation measurements agree within 1 %. We also demonstrate both online and offline measurements of plant trace gas exchange using the LI-6800. Offline measurements by pre-concentration on adsorbent cartridges enable detection of a broad suite of VOCs, including monoterpenes (e.g., limonene) and aldehydes (e.g., decanal). Online measurements can be more challenging if flow rates require dilution with ultra-pure zero air. We use high resolution time-of-flight chemical ionization mass spectrometry coupled to the LI-6800 to measure direct plant emission of formic acid.

1 Introduction

Non-methane volatile organic compounds (VOCs) are readily oxidized in the atmosphere and thus impact atmospheric composition, climate and human health. As such, a quantitative understanding of VOC sources is essential for predicting future air quality and climate conditions. VOC oxidation impacts greenhouse gas concentration by both producing tropospheric ozone and lowering OH radical concentrations, thereby increasing the lifetime of atmospheric methane (Kesselmeier and Staudt, 1999). Oxidized products of VOC precursors contribute to secondary organic aerosol (Faiola et al., 2018), which impacts climate and human health (Davidson et al., 2005; Pope III and Dockery, 2006). Biogenic emissions from plants dominate the global VOC source (Guenther et al., 1995; Lamarque et al., 2010; Lathière et al., 2006); terrestrial ecosystems and the ocean emit 1150 TgC yr^{-1} of VOCs globally (Guenther et al., 1995), relative to anthropogenic VOC sources, which account for only 142 TgC yr^{-1} globally (Singh, 1995). The most abundant group of biogenic VOCs (hereafter

https://doi.org/10.5194/amt-2020-45
Preprint. Discussion started: 25 March 2020


Atmospheric Measurement Techniques Discussions

"BVOCs") are isoprenoids (Kesselmeier and Staudt, 1999), molecules comprised of $(C_5H_8)_n$ units. Isoprene (C_5H_8) contributes to roughly half of global BVOC emissions, while monoterpenes ($C_{10}H_{16}$) and sesquiterpenes ($C_{15}H_{24}$) account for an additional 18% combined (Guenther et al., 2012).

BVOC emissions are affected by a complex combination of factors, including temperature (Tingey et al., 1980; Duhl et al., 2008; Tarvainen et al., 2005; Sharkey and Yeh, 2001), soil moisture (Ebel et al., 1995; Ormeño et al., 2007; Sharkey and Loreto, 1993), light (Tarvainen et al., 2005; Sharkey and Loreto, 1993; Owen et al., 2002; Staudt and Seufert, 1995), CO_2 concentration (Wilkinson et al., 2009; Loreto and Schnitzler, 2010), plant developmental stage (Holopainen, 2004; Kim et al., 2005; Zhang and Chen, 2009; Guenther, 1997), mechanical stress (Kaser et al., 2013a; Markovic et al., 2016), and biotic stress (Mauck et al., 2010; Niinemets et al., 2013; Scala et al., 2013). While the effects of some environmental factors, such as temperature, are well-understood, the effects of other factors, such as CO_2 concentration, are less clear. Different VOCs also have different temperature responses, and different plant species have different temperature responses for the same VOC. While most VOC emissions increase exponentially with a linear increase in temperature (Tingey et al., 1990; Peñuelas and Llusià, 2001; Niinemets et al., 2004) before reaching a maximum and rapidly decreasing (Grote et al., 2013), others are not sensitive with temperature (e.g., cis-β-ocimene) (Loreto et al., 1998). Temperature effects on VOC emissions are included in emission models, typically based on the results of short-term exposure experiments (Guenther et al., 1993; Guenther et al., 2012). Unlike temperature, the effect of changing CO_2 concentrations on BVOC emissions is under debate, even among plants of the same species (Loreto and Schnitzler, 2010). Under elevated CO_2 conditions, some studies observe no change in emissions (Constable et al., 1999; Kainulainen et al., 1998; Räisänen et al., 2008; Rapparini et al., 2003), while others observe a decrease (Scholefield et al., 2004; Sallas et al., 2003; Snow et al., 2003) or increase (Staudt et al., 2001a) in VOC emissions relative to ambient CO_2. Despite its importance to atmospheric composition, biogenic VOC emission response to environmental change remains poorly understood.

Global emission inventories of BVOCs vary across models (Arneth et al., 2008; Grote et al., 2013). Monoterpenes are treated less consistently than isoprene: the standard deviation of monoterpene emissions across multiple emission models is 40% of the mean, compared to 10% for isoprene (Arneth et al., 2008). Emission models that group several VOCs together, such as the monoterpene isomers, may simplify the model, but this approach assumes that emissions are similar across the isomeric class and neglects differences in atmospheric reactivities of compounds. For example, the lifetime for reaction with O_3 between α-pinene and β-pinene differ between a few hours to a day (Atkinson and Arey, 2003), which consequently affects the SOA yield (Friedman and Farmer, 2018). Some models use plant photosynthesis to predict VOC emissions (Grote et al., 2013; Grote et al., 2014), though the correlation between plant physiology and VOC emission – let alone the response of these parameters to external environmental stressors – is not well understood. Model limitations are due, in part, to the limited availability of measurements, particularly simultaneous measurements of plant physiology and speciated VOC emissions.

https://doi.org/10.5194/amt-2020-45
Preprint. Discussion started: 25 March 2020


Atmospheric Measurement Techniques Discussions

VOC emissions are commonly quantified through canopy measurements (e.g., Goldstein et al., 2004; Rinne et al., 2007; Kaser et al., 2013b; Ciccioli et al., 1999) and leaf or branch chamber headspace measurements (e.g., Kessler and Baldwin, 2001; Llusià et al., 2002; Komenda et al., 2001; Guenther et al., 2000). One approach to leaf-level studies couples a portable photosynthesis system (PPS) with a trace-gas analyzer, thus enabling simultaneous physiology and VOC emissions measurements (e.g. Lerdau and Keller, 1997; Brilli et al., 2007; Singsaas et al., 1999; Loreto and Velikova, 2001; Geron et al., 2006b; Brilli et al., 2011; Harley et al., 2014). The user can clamp the cuvette of the PPS onto a leaf and thereby control leaf-level parameters such as light wavelength and intensity, leaf temperature, humidity, air flow, and CO_2. Within the PPS, two infrared gas analyzers (IRGAs) determine the difference in gas concentration of CO_2 and water before and after the leaf cuvette. The system calculates physiological parameters including CO_2 assimilation rate (A), transpiration and stomatal conductance (for detailed calculations, refer to LI-COR, 2017). The CO_2 assimilation rate refers to the rate of photosynthetic CO_2 uptake into the leaf, transpiration is the rate at which water vapor is released from a leaf, and stomatal conductance is the rate at which CO_2 and water pass through the stomata of a leaf. Diverting the PPS air flow to an external gas analyzer enables users to sample leaf emissions. Emissions analysis can be both *in situ* and real-time if online detection techniques are available, such as proton transfer reaction mass spectrometry (PTR-MS; e.g. Brilli et al., 2011; Brilli et al., 2007; Harley et al., 2014) or portable gas chromatography (e.g., Geron et al., 2006b; Lerdau and Keller, 1997; Singsaas et al., 1999; Loreto and Velikova, 2001). However, gas samples can also be collected for offline analysis by thermal desorption gas chromatography mass spectrometry (e.g., Geron et al., 2006b; Harley et al., 2014) and gas chromatography mass spectrometry canister analysis (e.g., Geron et al., 2006a). These PPS-coupled techniques allow users to simultaneously obtain plant photosynthesis metrics and leaf-level VOC emissions.

While the PPS-VOC sampling technique has been used for decades, recent developments in PPSs provide new opportunities for leaf-level BVOC emission studies. The expanded ability to control environmental parameters, including leaf vapour pressure deficit, provides ample opportunity to study the connection between plant physiology and emission. However, PPS systems have not been rigorously evaluated in the literature for leaf-level emissions. Here, we characterize the recently developed LI-6800 portable photosynthesis system for leaf-level emissions, quantifying the capabilities and limitations of this method. We investigate the instrumental limits of this approach, including acceptable flow rates and best practices. We demonstrate the utility of this technique for offline measurements using thermal desorption gas chromatography mass spectrometry and online measurements using time-of-flight chemical ionization mass spectrometry.

2 Instrumentation

We use a commercial portable photosynthesis system (LI-6800) with a Multiphase Flash™ Fluorometer (LI-COR, Nebraska) for CO_2 and H_2O gas exchange measurements. The PPS consists of two major components: the console, which includes the

https://doi.org/10.5194/amt-2020-45
Preprint. Discussion started: 25 March 2020


Atmospheric Measurement Techniques Discussions

digital interface and the chemical columns for control of air composition; and the head, which contains the 6 cm^2 leaf chamber and controls leaf temperature. The LI-6800 PPS controls environmental conditions at the leaf level, including: temperature, humidity, light intensity and wavelength, and CO_2. The PPS also controls air flow and fan speed. As described in the Introduction, the PPS uses IRGAs to detect gas concentrations of CO_2 and water from before (reference, REF) and after (sample, SAM) the leaf chamber. The LI-6800 PPS has ports on both of these sample lines; air collected from the REF subsampling port can be used as a system background for emissions that do not occur within the PPS itself, while air collected from the SAM port is representative of leaf emissions and the system background. In instances where the analytes of interest are only emitted by plant tissue and not by the PPS, measurements taken from the REF port can be used to subtract background from the SAM port samples.

We define our standard operating conditions in Table 1, along with the technical capabilities of the instrument and the acceptable range determined herein. We acquired response curves by altering a single environmental parameter (e.g., temperature), waiting for leaf photosynthesis (i.e. CO_2 assimilation) to stabilize to new conditions, and then collecting gas exchange and VOC measurements. To determine the parameters for photosynthesis stabilization, we monitored a leaf using the PPS for 20 minutes, and determined the natural variability in stomatal conductance and CO_2 assimilation. A standard deviation limit can be set for the stability parameters, but we found the natural variability in our citrus plants changes daily. Therefore, we determined stability using a limit on the slope of stomatal conductance (0.01 mol m^{-2} s^{-1} min^{-1}) and CO_2 assimilation (0.5 μmol m^{-2} s^{-1} min^{-1}) measurements over a 15 second period. Photosynthesis stabilization took anywhere from 30 seconds to 15 minutes, depending on how close the set environmental conditions were to ambient or prior conditions. Unless otherwise noted, we controlled the LI-6800 input gas stream with a CO_2 scrubber (soda lime, LI-COR 9964-090), dessicant (blue-indicating Drierite, LI-COR 622-04299), humidifier (Stuttgarter Masse, LI-COR 9968-165), and CO_2 (8 g cartridges, LI-COR 9968-227 and Leland 30404). The values for flow rate and chemical conditions are in Table 1; further details on the instrument specifications, including component precision, can be found in the instrument manual (LI-COR, 2017).

Note that the LI-6800 denotes flow in terms of μmol s^{-1}. All flows are given in L min^{-1}; we performed experiments at 1525 m above sea level and use an air pressure of 0.844 atm for conversion calculations when necessary.

The flow path of the PPS subsampling system is shown in Fig. 1. Ambient air is pulled into the PPS through the air inlet between 1.18 and 2.96 L min^{-1} (680-1700 μmol s^{-1}), and is then treated for humidity and CO_2. The bulk flow is automatically calculated by the PPS software to control the user-defined parameter for chamber air flow (described in Table 1). A subsample of this ambient air flows through the REF IRGA and when in use, the REF subsampling port, while the remaining air enters the leaf chamber. Air exiting the leaf chamber is split between the SAM subsampling port and the second SAM IRGA. Air from the SAM and REF IRGAs is removed as exhaust through the main exhaust line. During emissions sampling,

https://doi.org/10.5194/amt-2020-45
Preprint. Discussion started: 25 March 2020


Atmospheric Measurement Techniques Discussions

the subsampling ports of the PPS can be simultaneously connected to trace gas analyzers, or alternated between a single analyzer with the other subsampling port closed. The air flow drawn out of the subsampling ports vary depending on emission sampling technique, and is described in more detail in Sect. 2.2.

The LI-6800 can be used with both online and offline emission sampling techniques. We use a chemical ionization mass spectrometer (CIMS) and an external CO_2 detector for online sampling, but note that the principles of flow rate control are easily generalized for other trace gas analysis including PTR-MS. We use thermal desorption gas chromatography mass spectrometry for offline analysis. These systems are described in detail below.

2.1 Portable Photosynthesis System

The PPS consists of the head (i.e., the device which clamps onto a leaf) (Fig. 2) and the console (i.e., the device which regulates environmental conditions and chemical use). The leaf chamber (Fig. 2A) was left unchanged while trace gas detector manifolds were connected to the SAM and REF subsampling ports (Fig. 2B and 2C, respectively). A 3.175 mm brass hose barb fitting is attached to each of the subsampling ports, followed by a 38 mm piece of flexible tubing (Tygon™, 6.35 mm o.d., 3.175 mm i.d.) that connects to a 1/4" stainless steel tee (Ultra-Torr). On each of the remaining ports (one perpendicular (Fig. $2B_2$, C_2) and one lateral (Fig. $2B_1$, C_1)), a 38 mm piece of polytetrafluoroethylene (PTFE) tubing (6.35 mm o.d., 3.175 mm i.d.) connects to a 6.35 mm perfluoroalkoxy alkane (PFA) fitting. The PFA fittings are capped unless actively used. For sorbent tube sampling, a cap on the lateral port (Fig. $2B_1$ for SAM, C_1 for REF) is replaced with a 6.35 mm fitting, and the sorbent tube (Fig. 2D) is fit directly in line. The external pump (Fig. 2E) ensures constant flow through the sorbent tube.

When subsampling the PPS air for BVOC emissions, an external pump subsamples air through the REF and/or SAM subsampling ports. The external pump ensures constant flow through the BVOC measurement system. The bulk flow through the system (F_I) is controlled by an internal pump in the console and any additional pumps used by trace gas analyzers on the REF or SAM subsampling ports. Thus the total air inlet flow is the sum of flows through REF port (F_R), SAM port (F_S) and the exhaust (F_E):

$$F_I = F_R + F_S + F_E \quad (1)$$

F_E includes flow from the internal REF and SAM IRGAs. The IRGAs each require at least 0.17 L min^{-1} (100 µmol s^{-1}) - though a flow above 0.35 L min^{-1} (200 µmol s^{-1}) is preferential - and the inlet flow can be a maximum of 2.96 L min^{-1} (1700 µmol s^{-1}). Due to the instrumental limitations of these flows, sampling flows (F_R and F_S) must not reach so high as to interfere with PPS system function. For thermal desorption sampling, where flow rates typically reach 0.2 L min^{-1}, samples can simultaneously be collected through both subsampling ports. The instrument will automatically calculate the split of flows between the IRGAs to account for system requirements. While higher flows (e.g., 1 L min^{-1}) can be sampled via the subsampling ports, the user will need to manually adjust the flow splits using the digital user interface on the console (LI-

https://doi.org/10.5194/amt-2020-45
Preprint. Discussion started: 25 March 2020


Atmospheric Measurement Techniques Discussions

COR, 2017). Using higher flow rates to accommodate sampling from the SAM port will impact the flow through the leaf chamber, and thus the conditions experienced by the leaf tissue. Impact of increased flow rates should be investigated for individual species.

2.2 Online measurements : TOF-CIMS

The PPS trace gas sampling scheme described above is well-suited for online trace gas detection. Here, we use two systems: (1) a CO2 analyzer and (2) a high resolution time-of-flight chemical ionization mass spectrometer (TOF-CIMS; Aerodyne Research Inc. and Tofwerk AG) (Brophy and Farmer, 2015) coupled to iodide reagent ions (Lee et al., 2014) to detect gas-phase formic acid. Details of the TOF-CIMS are in S1.

For external comparison of leaf CO_2 exchange with the internal IRGAs, we use an external CO_2 analyzer (LI-840A, Li-Cor, Nebraska), which was alternately connected to the REF and the SAM subsampling ports. The LI-840A analyzer requires 1L min^{-1} of flow.

The TOF-CIMS pulls 1.9 L min^{-1}, exceeding the maximum threshold for the PPS subsampling ports. To decrease the flow, we dilute the subsampled air with 2.00 ± 0.05 L min^{-2} of ultra-high purity zero air (UZA; Airgas) at the inlet to the CIMS. The diluting flow is controlled by a mass flow controller (MKS Instruments, Mass Flo® Controller, 1179B).

We calculate formic acid emission rates as follows:

$$C_P = C_C * \frac{Q_C}{Q_P} \quad (2)$$

where C_P is the concentration of the VOC coming from the PPS (mol mol^{-1}), C_C is the concentration of the VOC identified by the CIMS (mol mol^{-1}), Q_C is the total flow pulled by the CIMS (L min^{-1}), and Q_P is the flow taken from the PPS subsampling port (L min^{-1}). To get C_C, a calibration is used to convert integrated peak area into concentration; the resulting value is then divided by the time over which the integration occurred.

We then convert the leaf chamber flow (Q_L) from L min^{-1} to mol min^{-1} using:

$$Q_L(mol\ min^{-1}) = \frac{Q_L(L\ min^{-1})*P}{R*T} \quad (3)$$

where P is atmospheric pressure, R is the gas constant, and T is air temperature. Using equations 2 and 3, we obtain:

$$E_{VOC} = \frac{C_P*Q_L}{S} \quad (4)$$

where E_{VOC} is the VOC emission rate (mol m^{-2} min^{-1}), and S is the leaf area (m^2).

https://doi.org/10.5194/amt-2020-45
Preprint. Discussion started: 25 March 2020


Atmospheric Measurement Techniques Discussions

2.3 Offline detection: sorbent tubes

Thermal desorption (TD) gas chromatography mass spectrometry (GC/MS) is an offline sampling technique commonly used to sample atmospheric volatile and semi-volatile organic compounds (Harper, 2000). This technique pre-concentrates trace gases on sorbent tubes, which are stainless steel or glass tubes of specific dimensions that are filled with adsorbent materials. Different adsorbents target different analytes. Tenax TA is a general adsorbent, which has a sampling range of 7 to 26 carbons (C_7-C_{26}), and is relatively hydrophobic (Dettmer and Engewald, 2002). Other adsorbents, such as carbon molecular sieves (e.g., Carboxen 563) collect smaller molecules (C_2-C_5), but are sensitive to atmospheric humidity (Dettmer and Engewald, 2002). As air flows through the sorbent tubes, atmospheric constituents adsorb onto the surface. The tubes are then rapidly heated and the compounds thermally desorbed into an air stream for analysis by GC/MS.

Details of the TD-GC/MS method are in S2. Briefly, we use the TD-GC/MS with Tenax adsorbent cartridges to quantify seven monoterpenes, summarized in Table 2.

We calculate leaf-level VOC emissions from the cartridge samples as follows:

$$E_{VOC} = \frac{m_{VOC} * Q_L}{V * S} \quad (5)$$

where E_{VOC} is the VOC Emission rate (ng m^{-2} min^{-1}); m_{VOC} is the mass of the VOC (ng), as determined by the thermal desorption calibration; Q_L is the flow through the leaf chamber (L min^{-1}); V is the total volume of air sampled with the sorbent tube (L), sampling flow multiplied by sampling time; and S is the leaf surface area (m^2).

2.4 Sampling protocol

The sampling protocol involves clamping the PPS leaf chamber onto a leaf, waiting for the leaf to adapt to the leaf chamber conditions, collecting trace gas measurements from the SAM and REF subsampling ports, and then either removing the leaf chamber and moving to a new leaf (single emission point), or changing the environmental conditions to investigate leaf-level emissions responses to temperature, light, relative humidity, or CO_2 (Table 1). Photosynthesis may be measured simultaneously at any point in the sampling protocol, and is independent of emission measurements.

Once the PPS has undergone its standard warmup (≤45 min), we set the PPS to the standard environmental conditions and allow the instrument to equilibrate without a leaf present, with the leaf chamber closed (<15 min; the further the ambient conditions deviate from standard conditions, the longer the instrument takes to equilibrate). We match the IRGAs to one another (LI-COR, 2017) prior to collecting an emissions measurement, when the CO_2 or humidity values change, or within an hour since the last match. To collect a system background ('system blank'), we connect a sorbent tube to the SAM subsampling port and use an external handheld pump to sample emissions (0.2 L min^{-1}; 20 minutes). The tube is then removed and the subsampling port capped. To sample leaf emissions, we enclose a leaf in the PPS chamber and allow the

https://doi.org/10.5194/amt-2020-45
Preprint. Discussion started: 25 March 2020


Atmospheric Measurement Techniques Discussions

leaf to acclimate at standard conditions (30 seconds to 35 minutes). A sorbent tube and external pump connected to the SAM subsampling port samples the leaf emissions (0.2 L min^{-1}; 20 minutes).

225

At this point, users may make continuous measurements, survey measurements, or response measurements. A continuous measurement allows for the subsequent measurement of the same leaf tissue at the same environmental conditions (i.e. one leaf throughout the day). A survey measurement allows for the measurement of multiple leaves under one set of environmental conditions (i.e. sampling emissions from multiple leaves on the same plant). Importantly, each time a leaf is
230 physically placed in the PPS chamber, it requires time (30 s – 35 min, depending on environmental conditions) to acclimate. A response measurement allows for the measurement of a single leaf at different environmental conditions (e.g. sampling emissions as a function of temperature).

Leaves must acclimate to new environmental conditions. However, the time required for a leaf to adapt to placement in the
235 chamber or changing environmental conditions is inconsistently reported in leaf-level photosynthesis studies. Some studies allow leaves to acclimate until photosynthesis reaches stability or steady-state (e.g., Bunce, 2008; Domurath et al., 2012), though those terms are often undefined. Some studies use an upper (e.g., Yang et al., 2010) or a lower (e.g., Lang et al., 2013) time limit to allow photosynthesis to reach stability. When exact equilibration times are mentioned, they vary greatly between perturbations and between studies. For emissions measurements, equilibration times of both photosynthesis and
240 BVOC emission must be considered. Using the CIMS, we determined that it takes 10-15 minutes for both photosynthesis and formic acid to reach stability after being clamped or after an environmental change.

We investigated the potential for VOCs in the leaf chamber to persist from one experiment to another, after the leaf has been removed, through adsorption on gaskets or chamber surfaces ("carryover"). Carryover can cause spuriously high emission
245 measurements. To investigate carryover, we collected a system blank (no leaf present; SAM port) before introducing a ponderosa lemon (*Citrus limon x Citrus medica*) leaf into the chamber for the next 8 hours at varying temperatures. Immediately after removing the leaf at the end of the day, we collected a second system blank (no leaf present; SAM port). This comparison showed no carryover of cis-β-ocimene, β-pinene or caryophyllene – but 27 % of the initial (i.e. leaf in chamber) observed citral signal persisted after the leaf was removed. Citral is a relatively low volatility compound,
250 highlighting the importance of considering carryover from previous experiments in calculating emissions of lower volatility analytes.

2.5 Leaf chamber conditions

The PPS control of environmental conditions enables acquisition of short-term response curves for trace gas emissions, which are typically used to parameterize biogenic VOC emissions in atmospheric chemical transport models. Table 1
255 summarizes the ranges in parameters we find to be feasible for each environmental parameter.

https://doi.org/10.5194/amt-2020-45
Preprint. Discussion started: 25 March 2020


Atmospheric Measurement Techniques Discussions

The PPS regulates CO_2 and light well. However, both temperature and humidity regulation in the PPS depend on the balance between ambient and desired conditions. Relative humidity is constrained so as to not reach condensing conditions, so the extent of RH control depends on the temperature of the leaf chamber. For example, when aiming for high PPS temperatures (>30 °C), the PPS can have difficulty simultaneously maintaining high (>50 %) RH. When ambient temperatures are low (<4 °C), the PPS is challenged to maintain RH >35 %. This instrumental challenge occurs because temperature control in the PPS is limited by the heat exchanger; as the heat exchanger approaches dew point, the PPS takes proactive measures and slows the heating or cooling of the system. We find two approaches to deal with PPS temperature/RH problems: (i) temperature may be set independently of humidity, or (ii) temperature may be ramped slowly while humidity is maintained.

Of all of the controllable environmental conditions, temperature takes the longest for the PPS to regulate (10 ± 2 minutes to warm an empty chamber from 33 to 18 °C). Cooling takes twice as long as heating, and introducing a leaf into the chamber increases time necessary to cool by 35 % and time necessary to heat by 26 %. External fans improved the chamber temperature control at higher ambient temperatures, as did placing ice packs beside the air-inlet, around the chemical tubes, beside the leaf chamber, and on the side of the head improves the temperature control.

The LI-6800 also enables direct control of leaf vapour pressure deficit, but achieving a large dynamic range in vapour pressure deficit is subject to the same constraints as simultaneously changing temperature and RH in the PPS.

3 Internal PPS versus external CO_2 measurements

The LI-6800 PPS internally measures leaf-level CO_2 exchange with the SAM and REF IRGAs as a core measurement, providing CO_2 assimilation (μmol m^{-2} s^{-1}). Assimilation provides a useful metric of validation against external leaf-level emissions, and we compare leaf-level CO_2 assimilation measured internally by the LI-6800 PPS and externally through the subsampling manifold and an external CO_2 analyzer. Here, we used the CO_2 assimilation of a basil leaf (*Ocimum basilicum*) to verify that the use of an external subsampling port supports the same values as the PPS's internal IRGA systems.

We connected an external CO_2 analyzer (LI-840A, LI-COR, Nebraska) to the PPS (no leaf) and varied the CO_2 concentration to determine the sensitivity of external CO_2 measurements (using the LI-840A) with the internal LI-6800 CO_2 measurements. The LI-6800 can control CO_2 concentration in one of two locations: before (REF) or in (SAM) the leaf chamber. First, we compare CO_2 measurements between the internal (LI-6800) and external (LI-840A) CO_2 analyzers. We internally controlled the REF CO_2 concentration and measured the subsequent CO_2 concentration externally though each subsampling port. We then controlled the SAM CO_2 concentration and repeated the external measurements. All comparison experiments showed a strong correlation between internal and external CO_2 measurements (R^2 > 0.9999). The controlled CO_2 concentration for

https://doi.org/10.5194/amt-2020-45
Preprint. Discussion started: 25 March 2020


Atmospheric Measurement Techniques Discussions

both experiments ranged from 0 through 1600 ppm. We found the external CO_2 measurement was 5.5 % higher than the internal measurement, which we attribute to systematic differences in instrument calibration (Fig. 3). We find no evidence of leaks at below-ambient CO_2 concentrations.

We then compared CO_2 assimilation (sampling with leaf) between the internal PPS determination and the external measurements accounting for observed flows, etc. This external CO_2 assimilation measurement and calculation approach parallels our coupled PPS+online sampling trace gas measurement, and provides validation of the sampling approach. For CO_2 assimilation comparisons, we controlled the SAM CO_2 concentration and monitored the REF CO_2 concentration externally. We accounted for the calibration offset between internal and external CO_2 detectors. With the external CO_2 analyzer connected to the REF subsampling port and a leaf in the chamber, we set the PPS CO_2 concentration to 200, 400, 600, 800, and 1000 µmol CO_2 mol^{-1}. The PPS measured photosynthesis 10 times within 10 minutes while we externally monitored CO_2 concentrations from the REF port (1 Hz).

We calculate CO_2 assimilation (A) as:

$$A = \frac{Q_{L,c}*\left([CO_2]_R - [CO_2]_S*\frac{1-[H_2O]_{R,c}}{1-[H_2O]_{S,c}}\right)}{S} \quad \text{(6, adapted from LI-COR, 2017)}$$

where $Q_{L,c}$ is the flow through the leaf chamber (µmol s^{-1}), multiplied by the leak correction factor (unitless, provided by the PPS); $[CO_2]_R$ and $[CO_2]_S$ is the concentration of CO_2 (µmol mol^{-1}), as determined by the REF and SAM infrared gas analyzers, respectively; $[H_2O]_{R,c}$ and $[H_2O]_{S,c}$ are the concentration of H_2O (mol mol^{-1}), as determined by the REF and SAM infrared gas analyzers, respectively; S is the leaf area (m^2). We take $[H_2O]_{R,c}$ and $[H_2O]_{S,c}$ from the LI-6800.

The internally and externally calculated CO_2 assimilations correlate well (r^2 = 0.97) with 1 % difference between the two approaches (Fig. 3).

4 Trace gas backgrounds in the PPS

Background contamination reduces analyte signal accuracy. Co-eluting peaks in a gas chromatogram add additional difficulty in determining the exact peak area of a VOC analyte. When a chromatogram features heavy background contamination from a system, the chromatograms can become busy, challenging untargeted peak identification. Here we investigate the background VOCs in the PPS.

The REF port can be measured simultaneously with the SAM port to provide a background measurement of air entering the leaf chamber, but not any internal PPS sources of interferences in the leaf chamber.

https://doi.org/10.5194/amt-2020-45
Preprint. Discussion started: 25 March 2020


Atmospheric Measurement Techniques Discussions

The PPS is made of materials that can emit volatile compounds. While PPS system background may not contribute substantial background signals when using certain targeted analytical techniques (e.g., selected ion monitoring GC/MS), untargeted techniques, such as full scan GC/MS, are susceptible to background interference. TD-GC/MS chromatograms of the PPS (no leaf, 30 °C) revealed substantial background contamination, especially compared to the background of the Tenax tubes themselves (Fig. 4). The total integrated ion counts of identifiable peaks were 49 % higher background from the SAM port versus the REF, highlighting the problem of only using the REF port as a background for VOC analysis. These peak counts are substantially higher (by ~80 %) than the blank Tenax sorbent tube itself. Primary differences in the integrated peak area between SAM and REF are due to the five largest peaks, three of which are siloxanes. Siloxanes are commonly used in consumer products, including textiles, cosmetics, paint, and electronics (Fromme, 2018; Tilley and Fry, 2015), and were 41 % higher in the SAM than REF ports. The other two largest peaks are isobornyl acrylate (a film-forming agent) and n-octyl acrylate (an adhesive and coating component). While unlikely to interfere with leaf VOC emissions, co-elution with these peaks may lead to unidentified emissions in untargeted approaches. As a result of this work, we recommend taking frequent backgrounds from the SAM port to ensure no chamber background interference for anaytes of interest.

Figure 5 categorizes the signals from the SAM background by functional groups, highlighting the complexity and potential interferences for biogenic trace gas emission analysis. The large background signals caution against using bulk signal measurements (e.g. total observed carbon, or total observed reactivity) from the PPS without careful background analysis. Instead, targeted approaches like extracted ion chromatography (EIC) are a promising way to exclude spurious background signals. Figure 6 highlights the differences between the full chromatogram (total ion counts) and an EIC, where we selected for monoterpenes. This approach clearly separates leaf-emissions that are not present in the blank, including β-pinene (4.210 min), limonene (5.175 min) and β-ocimene (5.561 min). By minimizing background contamination with EIC, we clearly observe differences between strongly- and weakly-emitting leaves (Fig. 6). Therefore, we recommend an EIC approach for the semi-targeted identification and analysis of monoterpenes and aldehydes.

We investigated three approaches to minimizing the PPS backgrounds. We replaced the Drierite dessicant with silica gel orange (Sigma-Aldrich, 13767-2.5KG-R) and the Stuttgarter Masse humidifier with Perlite (Miracle Gro®, 74278430). We also installed fresh air filters at each chemical column, IRGA and the air-inlet. After each change, we flushed the system with heated air (35 °C at a flow rate of 1300 μmol s^{-1} for 30 minutes) before collecting system blanks under standard conditions, but none of these changes substantially decreased the background signals (Fig. S3).

The air entering the PPS is ambient, and thus prone to change with time. While the PPS includes several filters within the system, they do not filter all biogenic hydrocarbons – including monoterpenes. This is a particular problem in greenhouses, where low exchange rates, warm temperatures and large concentrations of plants lead to high ambient biogenic VOC

https://doi.org/10.5194/amt-2020-45
Preprint. Discussion started: 25 March 2020


Atmospheric Measurement Techniques Discussions

concentrations. We investigated the potential to filter monoterpenes from inlet air at the Plant Growth Facilities at Colorado State University. We added a home-built charcoal filter (30.5 cm piece of 85 cm o.d. stainless steel tubing filled with activated charcoal Norit® (Sigma-Aldrich, 29204-500G) and filtered with glass wool and stainless steel mesh on either end) to the air inlet of the PPS. This filter completely removed all background α-pinene from 0.04 ppb to below detection limit, but was less effective in subsequent outdoor experiments. As the ambient concentration of VOCs vary with time of day, we thus recommend both using a charcoal filter and taking simultaneous REF and SAM measurements to account for interferences from input air. Alternately, zero air can replace ambient input air at the PPS inlet, per manufacturer's instructions (LI-COR, 2017).

5 Case studies

Despite these background interferences, the LI-6800 has the potential to investigate plant gas exchange for an array of molecules with an array of trace gas instrumentation. Here, we provide case studies with both online (5.1; CIMS) and offline (5.2, 5.3; TD-GC-MS) analysis. TD offers the benefit in that the sorbent tubes are easily portable, though sample collection and analysis is timely. CIMS offers the benefit of online, real-time data acquisition, however the instrument itself is less portable and provides no definitive compound identities. These case studies maintained standard conditions unless otherwise noted, and each study used different plants.

5.1 Formic acid emissions

Organic acids account for roughly 25 % of global non-methane VOCs (Khare et al., 1999) and contribute to secondary organic aerosol (Yatavelli et al., 2014). Despite their ubiquity, models typically underestimate ambient concentrations of formic acid, even the structurally simplest of organic acids, implying a missing source (Paulot et al., 2011; Alwe et al., 2019). This missing source of formic acid is not soils (Mielnik et al., 2018), but flux studies (Fulgham et al., 2019) and vertical gradient measurements (Mattila et al., 2018) suggest a direct ecosystem source. Here we demonstrate the capacity of the PPS coupled to a CIMS system to investigate leaf-level organic acid sources.

We conducted a temperature response curve on a spearmint leaf (*Mentha spicata*) connected to the PPS with a CIMS detector. We performed three temperature response curve replicates, each with temperatures varying from 21 to 35 °C. The leaf was acclimated (as described in Sect. 2) at each new temperature for at least 5 minutes, during which time the CIMS sampled the REF port to determine the system background. We then simultaneously measured leaf-level emissions of formic acid and photosynthetic parameters for 5 minutes.

CO_2 assimilation and formic acid emission both varied with temperature for this leaf (Fig. 7). As temperature increases, CO_2 assimilation increases up to a maximum value of 14.2 μmol m^{-2} s^{-1} at 26 °C. This CO_2 assimilation follows the expected

https://doi.org/10.5194/amt-2020-45
Preprint. Discussion started: 25 March 2020


Atmospheric Measurement Techniques Discussions

cubic fit (Yamori et al., 2010). In contrast, formic acid continues to increase above the photosynthesis maximum, with maximum emission (49.9 nmol m^{-2} min^{-1}) occurring at 29 °C. However, we emphasize that this represents a single experiment using the CIMS to demonstrate the utility of coupling the CIMS to the PPS, rather than an extensive or replicated experiment of formic acid emissions. Thus, these observations should be considered a case study, rather than emissions ratios to be used in models. This case study does demonstrate the potential for the PPS to be coupled to real-time measurements in exploring less-studied BVOCs, such as organic acids, at a leaf level.

5.2 Decanal emissions

C_6 – C_{10} aldehydes are an understudied class of plant BVOC emissions (Ciccioli et al., 1993; Wildt et al., 2003; Owen et al., 1997). Aldehydes can contribute to free radical formation in the atmosphere through photolysis or reaction with OH radicals (Atkinson, 1986). Decanal (C_{10}-aldehyde) is present in atmospheric mixing ratios of ppt_v to ppb_v (Ciccioli et al., 1993), and is emitted by plants in response to stress (Wildt et al., 2003). Here, we demonstrate the potential for off-line measurements (i.e. the TD-GC/MS) coupled to the PPS to investigate plant emissions of C_6-C_{10} aldehydes. Figure 8 shows the temperature response curve of a single leaf on a basil plant (*Ocimum basilicum*) in lab. We collected single sorbent tubes for 20 minutes at each point as we varied temperature by ~3 °C from 18 to 35 °C. The LI-6800 simultaneously measured photosynthesis every 30 seconds.

CO_2 assimilation increases over the entire range of temperatures, beginning to stabilize around 33 °C. A cubic fit to assimilation suggests that 35 °C was the maxima in assimilation, which would decrease at higher temperatures. In contrast to photosynthesis, decanal exhibits bi-directional exchange. As temperature increases, decanal emissions are initially negative (i.e. lower than the background concentration of input air), and then show enhanced uptake with increasing temperature before a turn-over point at which emission rapidly increases. The temperature response is inconsistent with stored pools (Grote et al., 2013), suggesting a more complex biochemical pathway.

The observed uptake of decanal below 27 °C supports the idea of a turnover point and bidirectional exchange of VOCs (Niinemets et al., 2014; Millet et al., 2018). Further investigation of turnover points as a function of varying input air concentration are warranted.

Temperature response curves can be used to compare the thermotolerance between species or between plants of the same species. For example, this study suggests that basil has a higher photosynthetic thermotolerance than mint (Fig. 8 and Fig. 7), despite the fact that basil had a lower CO_2 assimilation rate. Comparing the emission of lesser-studied compounds like decanal to that of formic acid or monoterpenes can better inform of the impact and deciding factors in leaf-level BVOC emissions.

https://doi.org/10.5194/amt-2020-45
Preprint. Discussion started: 25 March 2020


Atmospheric Measurement Techniques Discussions

5.3 Monoterpene emissions

The PPS-coupled emission sampling method is portable, which we take advantage of in our third case study. While BVOC emission studies often quantify emissions in terms of dry leaf weight, *in situ* measurements enable us to collect data based on leaf area, which is used in many emissions models.

To investigate the difference in limonene and γ-terpinene emissions between plants of different species, we sampled two shaded leaves of each of three tree species during the summer of 2019 in the Colorado State University Arboretum in Fort Collins, CO. We sampled: *Ginkgo biloba* (ginkgo), *Morus alba* (mulberry), and *Juglans regia* (walnut). Emissions were taken at 27±2 °C, near-ambient CO_2 (414 ppm), and under saturating light conditions (2000 μmol m^{-2} s^{-1}). We simultaneously sampled monoterpene emissions using the sorbent cartridges (30 minute collection) and photosynthesis (30 second time resolution) at each temperature. Leaf temperature was difficult to regulate in the field. The PPS maintained a 25 °C leaf temperature with ambient temperatures up to 29 °C, but could not keep leaf temperatures below 28 °C when ambient temperatures increased, even with shading and ice packs.

Here, limonene emissions from all species were an order of magnitude greater than γ-terpinene, by factors of 10-20 (Fig. 9). Within leaves of a single plant, chamber temperature and subsequent CO_2 assimilation rates were similar (<0.5 % difference in assimilation between leaves of the same plant), but monoterpene emission rates from individual leaves varied, though this variance was more notable for γ-terpinene than limonene. For example, limonene emission rates differed by 24 % between the two mulberry leaves, whereas γ-terpinene differed by 46 %. This discrepancy in variance between CO_2 assimilation and monoterpene emissions on a single plant highlights the limitation of tying modelled photosynthesis rates to VOC emissions and warrants further investigation. While limited to two monoterpenes here, this field survey approach to trace gas VOC emissions can provide a species-specific monoterpene emission cassette. These case study data support that leaf emissions can vary between leaves of one tree (Staudt et al., 2001b), between trees of one species (Staudt et al., 2001b), and between trees of different species (Benjamin et al., 1996) – but that trace gas sampling with the PPS is a viable method for investigating these sources of variance.

6 Conclusions

This study shows the utility of a new PPS system coupled with both on- and off-line analysis for the analysis of leaf-level gas emissions, and the limitation and caveats associated with those measurements. In particular, trace gas measurements with high air flow needs (> 1 L min^{-1}) must be used carefully. Using an external CO_2 monitor to calculate CO_2 assimilation rates, we verify the integrity of the subsampling manifold and provide relevant equations for calculations of plant gas exchange.

https://doi.org/10.5194/amt-2020-45
Preprint. Discussion started: 25 March 2020


Atmospheric Measurement Techniques Discussions

The PPS-coupling system described herein has substantial potential for improving our understanding of plant emissions. For example, different CIMS ionization sources can target different types of organic molecules (e.g. acetate ionization for organic acids vs iodide ionization for oxygenated organics), and different sorbent materials in thermal desorption tubes enable detection of different compounds (i.e. Tenax for monoterpenes vs graphitic carbon for isoprene). However, we emphasize the importance of carefully considering potential contaminants from the PPS itself, and the use of frequent system background measurements through both the SAM port in the absence of a leaf, and the REF port in presence of the leaf. The further potential to control the composition of the airflow into the PPS will enable investigation of compensation points.

References

Alwe, H. D., Millet, D. B., Chen, X., Raff, J. D., Payne, Z. C., and Fledderman, K.: Oxidation of volatile organic compounds as the major source of formic acid in a mixed forest canopy, Geophys Res Lett, 46, 2940-2948, 2019.

Arneth, A., Monson, R., Schurgers, G., Niinemets, Ü., and Palmer, P.: Why are estimates of global terrestrial isoprene emissions so similar (and why is this not so for monoterpenes)?, Atmos Chem Phys, 8, 4605-4620, 2008.

Atkinson, R.: Kinetics and mechanisms of the gas-phase reactions of the hydroxyl radical with organic compounds under atmospheric conditions, Chem Rev, 86, 69-201, 1986.

Atkinson, R., and Arey, J.: Gas-phase tropospheric chemistry of biogenic volatile organic compounds: a review, Atmospheric Environment, 37, 197-219, 2003.

Benjamin, M. T., Sudol, M., Bloch, L., and Winer, A. M.: Low-emitting urban forests: a taxonomic methodology for assigning isoprene and monoterpene emission rates, Atmospheric Environment, 30, 1437-1452, 1996.

Bernal, E.: Limit of detection and limit of quantification determination in gas chromatography, in: Advances in gas chromatography, IntechOpen, 2014.

Brilli, F., Barta, C., Fortunati, A., Lerdau, M., Loreto, F., and Centritto, M.: Response of isoprene emission and carbon metabolism to drought in white poplar (Populus alba) saplings, New Phytologist, 175, 244-254, 2007.

Brilli, F., Ruuskanen, T. M., Schnitzhofer, R., Müller, M., Breitenlechner, M., Bittner, V., Wohlfahrt, G., Loreto, F., and Hansel, A.: Detection of plant volatiles after leaf wounding and darkening by proton transfer reaction "time-of-flight" mass spectrometry (PTR-TOF), PLoS One, 6, e20419, 2011.

Brophy, P., and Farmer, D.: A switchable reagent ion high resolution time-of-flight chemical ionization mass spectrometer for real-time measurement of gas phase oxidized species: characterization from the 2013 southern oxidant and aerosol study, Atmos Meas Tech, 8, 2945-2959, 2015.

Bunce, J.: Acclimation of photosynthesis to temperature in Arabidopsis thaliana and Brassica oleracea, Photosynthetica, 46, 517-524, 2008.

https://doi.org/10.5194/amt-2020-45
Preprint. Discussion started: 25 March 2020


Atmospheric Measurement Techniques Discussions

Ciccioli, P., Brancaleoni, E., Frattoni, M., Cecinato, A., and Brachetti, A.: Ubiquitous occurrence of semi-volatile carbonyl compounds in tropospheric samples and their possible sources, Atmospheric Environment. Part A. General Topics, 27, 1891-1901, 1993.

Ciccioli, P., Brancaleoni, E., Frattoni, M., Di Palo, V., Valentini, R., Tirone, G., Seufert, G., Bertin, N., Hansen, U., and Csiky, O.: Emission of reactive terpene compounds from orange orchards and their removal by within-canopy processes, Journal of Geophysical Research: Atmospheres, 104, 8077-8094, 1999.

Constable, J. V., Litvak, M. E., Greenberg, J. P., and Monson, R. K.: Monoterpene emission from coniferous trees in response to elevated CO2 concentration and climate warming, Global Change Biology, 5, 252-267, 1999.

Davidson, C. I., Phalen, R. F., and Solomon, P. A.: Airborne particulate matter and human health: A review, Aerosol Sci Tech, 39, 737-749, 2005.

Dettmer, K., and Engewald, W.: Adsorbent materials commonly used in air analysis for adsorptive enrichment and thermal desorption of volatile organic compounds, Analytical and bioanalytical chemistry, 373, 490-500, 2002.

Domurath, N., Schroeder, F.-G., and Glatzel, S.: Light response curves of selected plants under different light conditions, VII International Symposium on Light in Horticultural Systems 956, 2012, 291-298,

Duhl, T., Helmig, D., and Guenther, A.: Sesquiterpene emissions from vegetation: a review, 2008.

Ebel, R. C., Mattheis, J. P., and Buchanan, D. A.: Drought stress of apple trees alters leaf emissions of volatile compounds, Physiologia Plantarum, 93, 709-712, 1995.

Faiola, C. L., Buchholz, A., Kari, E., Yli-Pirilä, P., Holopainen, J. K., Kivimäenpää, M., Miettinen, P., Worsnop, D. R., Lehtinen, K. E. J., Guenther, A. B., and Virtanen, A.: Terpene Composition Complexity Controls Secondary Organic Aerosol Yields from Scots Pine Volatile Emissions, Scientific Reports, 8, 3053, 10.1038/s41598-018-21045-1, 2018.

Friedman, B., and Farmer, D. K.: SOA and gas phase organic acid yields from the sequential photooxidation of seven monoterpenes, Atmospheric environment, 187, 335-345, 2018.

Fromme, H.: Cyclic Volatile Methylsiloxanes: Occurrence and Exposure, 2018.

Fulgham, S. R., Brophy, P., Link, M., Ortega, J., Pollack, I., and Farmer, D. K.: Seasonal flux measurements over a Colorado pine forest demonstrate a persistent source of organic acids, ACS Earth and Space Chemistry, 3, 2017-2032, 2019.

Geron, C., Guenther, A., Greenberg, J., Karl, T., and Rasmussen, R.: Biogenic volatile organic compound emissions from desert vegetation of the southwestern US, Atmospheric Environment, 40, 1645-1660, 2006a.

Geron, C., Owen, S., Guenther, A., Greenberg, J., Rasmussen, R., Bai, J. H., Li, Q.-J., and Baker, B.: Volatile organic compounds from vegetation in southern Yunnan Province, China: Emission rates and some potential regional implications, Atmospheric Environment, 40, 1759-1773, 2006b.

Goldstein, A., McKay, M., Kurpius, M., Schade, G., Lee, A., Holzinger, R., and Rasmussen, R.: Forest thinning experiment confirms ozone deposition to forest canopy is dominated by reaction with biogenic VOCs, Geophys Res Lett, 31, 2004.

Grote, R., Monson, R. K., and Niinemets, Ü.: Leaf-level models of constitutive and stress-driven volatile organic compound emissions, in: Biology, controls and models of tree volatile organic compound emissions, Springer, 315-355, 2013.

https://doi.org/10.5194/amt-2020-45
Preprint. Discussion started: 25 March 2020

Grote, R., Morfopoulos, C., Niinemets, Ü., Sun, Z., Keenan, T. F., Pacifico, F., and Butler, T.: A fully integrated isoprenoid emissions model coupling emissions to photosynthetic characteristics, Plant, cell & environment, 37, 1965-1980, 2014.

Guenther, A., Hewitt, C. N., Erickson, D., Fall, R., Geron, C., Graedel, T., Harley, P., Klinger, L., Lerdau, M., and McKay, W.: A global model of natural volatile organic compound emissions, Journal of Geophysical Research: Atmospheres, 100, 8873-8892, 1995.

Guenther, A.: Seasonal and spatial variations in natural volatile organic compound emissions, Ecological applications, 7, 34-45, 1997.

Guenther, A., Geron, C., Pierce, T., Lamb, B., Harley, P., and Fall, R.: Natural emissions of non-methane volatile organic compounds, carbon monoxide, and oxides of nitrogen from North America, Atmospheric Environment, 34, 2205-2230, 2000.

Guenther, A., Jiang, X., Heald, C., Sakulyanontvittaya, T., Duhl, T., Emmons, L., and Wang, X.: The Model of Emissions of Gases and Aerosols from Nature version 2.1 (MEGAN2. 1): an extended and updated framework for modeling biogenic emissions, 2012.

Guenther, A. B., Zimmerman, P. R., Harley, P. C., Monson, R. K., and Fall, R.: Isoprene and monoterpene emission rate variability: model evaluations and sensitivity analyses, Journal of Geophysical Research: Atmospheres, 98, 12609-12617, 1993.

Harley, P., Eller, A., Guenther, A., and Monson, R. K.: Observations and models of emissions of volatile terpenoid compounds from needles of ponderosa pine trees growing in situ: control by light, temperature and stomatal conductance, Oecologia, 176, 35-55, 2014.

Harper, M.: Sorbent trapping of volatile organic compounds from air, Journal of Chromatography A, 885, 129-151, 2000.

Holopainen, J. K.: Multiple functions of inducible plant volatiles, Trends in plant science, 9, 529-533, 2004.

Kainulainen, P., Holopainen, J., and Holopainen, T.: The influence of elevated CO 2 and O 3 concentrations on Scots pine needles: changes in starch and secondary metabolites over three exposure years, Oecologia, 114, 455-460, 1998.

Kaser, L., Karl, T., Guenther, A., Graus, M., Schnitzhofer, R., Turnipseed, A., Fischer, L., Harley, P., Madronich, M., and Gochis, D.: Undisturbed and disturbed above canopy ponderosa pine emissions: PTR-TOF-MS measurements and MEGAN 2.1 model results, 2013a.

Kaser, L., Karl, T., Schnitzhofer, R., Graus, M., Herdlinger-Blatt, I., DiGangi, J., Sive, B., Turnipseed, A., Hornbrook, R., and Zheng, W.: Comparison of different real time VOC measurement techniques in a ponderosa pine forest, Atmos Chem Phys, 13, 2893-2906, 2013b.

Kesselmeier, J., and Staudt, M.: Biogenic volatile organic compounds (VOC): an overview on emission, physiology and ecology, Journal of atmospheric chemistry, 33, 23-88, 1999.

Kessler, A., and Baldwin, I. T.: Defensive function of herbivore-induced plant volatile emissions in nature, Science, 291, 2141-2144, 2001.

https://doi.org/10.5194/amt-2020-45
Preprint. Discussion started: 25 March 2020

Khare, P., Kumar, N., Kumari, K., and Srivastava, S.: Atmospheric formic and acetic acids: An overview, Reviews of geophysics, 37, 227-248, 1999.

Kim, J.-C., Kim, K.-J., Kim, D.-S., and Han, J.-S.: Seasonal variations of monoterpene emissions from coniferous trees of different ages in Korea, Chemosphere, 59, 1685-1696, 2005.

Komenda, M., Parusel, E., Wedel, A., and Koppmann, R.: Measurements of biogenic VOC emissions: sampling, analysis and calibration, Atmospheric environment, 35, 2069-2080, 2001.

Lamarque, J.-F., Bond, T. C., Eyring, V., Granier, C., Heil, A., Klimont, Z., Lee, D., Liousse, C., Mieville, A., and Owen, B.: Historical (1850–2000) gridded anthropogenic and biomass burning emissions of reactive gases and aerosols: methodology and application, Atmos Chem Phys, 10, 7017-7039, 2010.

Lang, Y., Wang, M., Zhang, G., and Zhao, Q.: Experimental and simulated light responses of photosynthesis in leaves of three tree species under different soil water conditions, Photosynthetica, 51, 370-378, 2013.

Lathière, J., Hauglustaine, D. A., Friend, A. D., De Noblet-Ducoudré, N., Viovy, N., and Folberth, G. A.: Impact of climate variability and land use changes on global biogenic volatile organic compound emissions, Atmos. Chem. Phys., 6, 2129-2146, 10.5194/acp-6-2129-2006, 2006.

Lee, B. H., Lopez-Hilfiker, F. D., Mohr, C., Kurtén, T., Worsnop, D. R., and Thornton, J. A.: An iodide-adduct high-resolution time-of-flight chemical-ionization mass spectrometer: Application to atmospheric inorganic and organic compounds, Environ Sci Technol, 48, 6309-6317, 2014.

Lerdau, M., and Keller, M.: Controls on isoprene emission from trees in a subtropical dry forest, Plant, Cell & Environment, 20, 569-578, 1997.

LI-COR: Using the LI-6800 Portable Photosynthesis System, 2017.

Llusià, J., Peñuelas, J., and Gimeno, B.: Seasonal and species-specific response of VOC emissions by Mediterranean woody plant to elevated ozone concentrations, Atmospheric Environment, 36, 3931-3938, 2002.

Loreto, F., Förster, A., Dürr, M., Csiky, O., and Seufert, G.: On the monoterpene emission under heat stress and on the increased thermotolerance of leaves of Quercus ilex L. fumigated with selected monoterpenes, Plant, Cell & Environment, 21, 101-107, 1998.

Loreto, F., and Velikova, V.: Isoprene produced by leaves protects the photosynthetic apparatus against ozone damage, quenches ozone products, and reduces lipid peroxidation of cellular membranes, Plant Physiology, 127, 1781-1787, 2001.

Loreto, F., and Schnitzler, J.-P.: Abiotic stresses and induced BVOCs, Trends in plant science, 15, 154-166, 2010.

Markovic, D., Nikolic, N., Glinwood, R., Seisenbaeva, G., and Ninkovic, V.: Plant responses to brief touching: a mechanism for early neighbour detection?, PloS one, 11, e0165742, 2016.

Mattila, J. M., Brophy, P., Kirkland, J., Hall, S., Ullmann, K., Fischer, E. V., Brown, S., McDuffie, E., Tevlin, A., and Farmer, D. K.: Tropospheric sources and sinks of gas-phase acids in the Colorado Front Range, 2018.

Mauck, K. E., De Moraes, C. M., and Mescher, M. C.: Deceptive chemical signals induced by a plant virus attract insect vectors to inferior hosts, Proceedings of the National Academy of Sciences, 107, 3600-3605, 2010.

Mielnik, A., Link, M., Mattila, J., Fulgham, S. R., and Farmer, D. K.: Emission of formic and acetic acids from two Colorado soils, Environmental Science: Processes & Impacts, 20, 1537-1545, 2018.

Millet, D. B., Alwe, H. D., Chen, X., Deventer, M. J., Griffis, T. J., Holzinger, R., Bertman, S. B., Rickly, P. S., Stevens, P. S., and Léonardis, T.: Bidirectional ecosystem–atmosphere fluxes of volatile organic compounds across the mass spectrum: How many matter?, ACS Earth and Space Chemistry, 2, 764-777, 2018.

Niinemets, Ü., Loreto, F., and Reichstein, M.: Physiological and physicochemical controls on foliar volatile organic compound emissions, Trends in plant science, 9, 180-186, 2004.

Niinemets, Ü., Kännaste, A., and Copolovici, L.: Quantitative patterns between plant volatile emissions induced by biotic stresses and the degree of damage, Frontiers in Plant Science, 4, 262, 2013.

Niinemets, Ü., Fares, S., Harley, P., and Jardine, K. J.: Bidirectional exchange of biogenic volatiles with vegetation: emission sources, reactions, breakdown and deposition, Plant, cell & environment, 37, 1790-1809, 2014.

Ormeño, E., Mevy, J., Vila, B., Bousquet-Mélou, A., Greff, S., Bonin, G., and Fernandez, C.: Water deficit stress induces different monoterpene and sesquiterpene emission changes in Mediterranean species. Relationship between terpene emissions and plant water potential, Chemosphere, 67, 276-284, 2007.

Owen, S., Boissard, C., Street, R., Duckham, S., Csiky, O., and Hewitt, C.: Screening of 18 Mediterranean plant species for volatile organic compound emissions, Atmospheric Environment, 31, 101-117, 1997.

Owen, S., Harley, P., Guenther, A., and Hewitt, C.: Light dependency of VOC emissions from selected Mediterranean plant species, Atmospheric environment, 36, 3147-3159, 2002.

Paulot, F., Wunch, D., Crounse, J. D., Toon, G., Millet, D. B., DeCarlo, P. F., Vigouroux, C., Deutscher, N. M., González Abad, G., and Notholt, J.: Importance of secondary sources in the atmospheric budgets of formic and acetic acids, Atmos Chem Phys, 11, 1989-2013, 2011.

Peñuelas, J., and Llusià, J.: The complexity of factors driving volatile organic compound emissions by plants, Biologia Plantarum, 44, 481-487, 2001.

Pope III, C. A., and Dockery, D. W.: Health effects of fine particulate air pollution: lines that connect, J Air Waste Manage, 56, 709-742, 2006.

Räisänen, T., Ryyppö, A., and Kellomäki, S.: Effects of elevated CO2 and temperature on monoterpene emission of Scots pine (Pinus sylvestris L.), Atmospheric Environment, 42, 4160-4171, 2008.

Rapparini, F., Baraldi, R., Miglietta, F., and Loreto, F.: Isoprenoid emission in trees of Quercus ilex with lifetime exposure to naturally high CO2 environment, Plant, Cell & Environment, 2003.

Rinne, J., Taipale, R., Markkanen, T., Ruuskanen, T., Hellén, H., Kajos, M., Vesala, T., and Kulmala, M.: Hydrocarbon fluxes above a Scots pine forest canopy: measurements and modeling, Atmos Chem Phys, 7, 3361-3372, 2007.

Sallas, L., Luomala, E.-M., Utriainen, J., Kainulainen, P., and Holopainen, J. K.: Contrasting effects of elevated carbon dioxide concentration and temperature on Rubisco activity, chlorophyll fluorescence, needle ultrastructure and secondary metabolites in conifer seedlings, Tree Physiol, 23, 97-108, 2003.

https://doi.org/10.5194/amt-2020-45
Preprint. Discussion started: 25 March 2020


Atmospheric Measurement Techniques Discussions

Scala, A., Allmann, S., Mirabella, R., Haring, M., and Schuurink, R.: Green leaf volatiles: a plant's multifunctional weapon against herbivores and pathogens, International journal of molecular sciences, 14, 17781-17811, 2013.

Scholefield, P., Doick, K., Herbert, B., Hewitt, C. S., Schnitzler, J. P., Pinelli, P., and Loreto, F.: Impact of rising CO2 on emissions of volatile organic compounds: isoprene emission from Phragmites australis growing at elevated CO2 in a natural carbon dioxide spring, Plant, Cell & Environment, 27, 393-401, 2004.

Sharkey, T. D., and Loreto, F.: Water stress, temperature, and light effects on the capacity for isoprene emission and photosynthesis of kudzu leaves, Oecologia, 95, 328-333, 1993.

Sharkey, T. D., and Yeh, S.: Isoprene emission from plants, Annual review of plant biology, 52, 407-436, 2001.

Singh, H. B.: Composition, chemistry, and climate of the atmosphere, Van Nostrand Reinhold Company, 1995.

Singsaas, E. L., Laporte, M. M., Shi, J.-Z., Monson, R. K., Bowling, D. R., Johnson, K., Lerdau, M., Jasentuliytana, A., and Sharkey, T. D.: Kinetics of leaf temperature fluctuation affect isoprene emission from red oak (Quercus rubra) leaves, Tree Physiol, 19, 917-924, 1999.

Snow, M. D., Bard, R. R., Olszyk, D. M., Minster, L. M., Hager, A. N., and Tingey, D. T.: Monoterpene levels in needles of Douglas fir exposed to elevated CO2 and temperature, Physiologia Plantarum, 117, 352-358, 2003.

Staudt, M., and Seufert, G.: Light-dependent emission of monoterpenes by holm oak (Quercus ilex L.), Naturwissenschaften, 82, 89-92, 1995.

Staudt, M., Joffre, R., Rambal, S., and Kesselmeier, J.: Effect of elevated CO2 on monoterpene emission of young Quercus ilex trees and its relation to structural and ecophysiological parameters, Tree Physiol, 21, 437-445, 2001a.

Staudt, M., Mandl, N., Joffre, R., and Rambal, S.: Intraspecific variability of monoterpene composition emitted by Quercus ilex leaves, Canadian Journal of Forest Research, 31, 174-180, 2001b.

Tarvainen, V., Hakola, H., Hellén, H., Bäck, J., Hari, P., and Kulmala, M.: Temperature and light dependence of the VOC emissions of Scots pine, Atmos Chem Phys, 5, 989-998, 2005.

Tilley, S. K., and Fry, R. C.: Priority environmental contaminants: understanding their sources of exposure, biological mechanisms, and impacts on health, in: Systems Biology in Toxicology and Environmental Health, Elsevier, 117-169, 2015.

Tingey, D., Turner, D., and Weber, J.: Factors controlling the emissions of monoterpenes and other volatile organic compounds, Trace gas emission by plants., 93-119, 1990.

Tingey, D. T., Manning, M., Grothaus, L. C., and Burns, W. F.: Influence of light and temperature on monoterpene emission rates from slash pine, Plant Physiology, 65, 797-801, 1980.

Wildt, J., Kobel, K., Schuh-Thomas, G., and Heiden, A.: Emissions of oxygenated volatile organic compounds from plants Part II: emissions of saturated aldehydes, Journal of Atmospheric Chemistry, 45, 173-196, 2003.

Wilkinson, M. J., Monson, R. K., Trahan, N., Lee, S., Brown, E., Jackson, R. B., Polley, H. W., Fay, P. A., and Fall, R.: Leaf isoprene emission rate as a function of atmospheric CO2 concentration, Global Change Biology, 15, 1189-1200, 2009.

Yamori, W., Evans, J. R., and Von Caemmerer, S.: Effects of growth and measurement light intensities on temperature dependence of CO2 assimilation rate in tobacco leaves, Plant, Cell & Environment, 33, 332-343, 2010.

https://doi.org/10.5194/amt-2020-45
Preprint. Discussion started: 25 March 2020

Atmospheric Measurement Techniques Discussions

Yang, X., Wang, X., and Wei, M.: Response of photosynthesis in the leaves of cucumber seedlings to light intensity and CO2 concentration under nitrate stress, Turkish Journal of Botany, 34, 303-310, 2010.

Yatavelli, R., Stark, H., Thompson, S., Kimmel, J., Cubison, M., Day, D., Campuzano-Jost, P., Palm, B., Hodzic, A., and Thornton, J.: Semicontinuous measurements of gas–particle partitioning of organic acids in a ponderosa pine forest using a MOVI-HRToF-CIMS, Atmos Chem Phys, 14, 1527-1546, 2014.

Zhang, P., and Chen, K.: Age-dependent variations of volatile emissions and inhibitory activity toward Botrytis cinerea and Fusarium oxysporum in tomato leaves treated with chitosan oligosaccharide, Journal of Plant Biology, 52, 332-339, 2009.

https://doi.org/10.5194/amt-2020-45
Preprint. Discussion started: 25 March 2020

Atmospheric Measurement Techniques Discussions

Table 1. User-defined standard, tested and operating conditions of environmental controls using the LI-6800.

	Chamber flow (µmol s^{-1})	Chamber overpressure (kPa)	Fan speed (rpm)	Relative humidity (%)	Photon Flux Density[c] (µmol m^{-2} s^{-1})	Temperature (°C)	CO_2 (µmol mol^{-1})
Standard conditions	500	0.1	10,000	50	750	25	400
Tested conditions[a]	0 – 1475	0.0 – 0.2	3,000 – 14,000	0 – 75%	0 – 3000	10 – 38	0 – 2000
Operating conditions[b]	0 – 1400[d]	0.0 – 0.2	10,000	0 – 90%	0 – 3000	± 10 from ambient	0 – 2000[e]

[a] Provided values indicate the range at which the instrument functioned properly in conditions tested at 1.5 km above sea level, ~0.84 atm (8.6 kPa).

[b] Recommended operating values from (LI-COR, 2017).

[c] Saturating light conditions recommended for most uses. Operating range dependent on temperature, values shown are for 25 °C.

[d] At standard ambient temperature (25 °C) and pressure (100 kPa, 0.99 atm).

[e] Exact values limited on bulk flow rate, review (LI-COR, 2017) for further details.

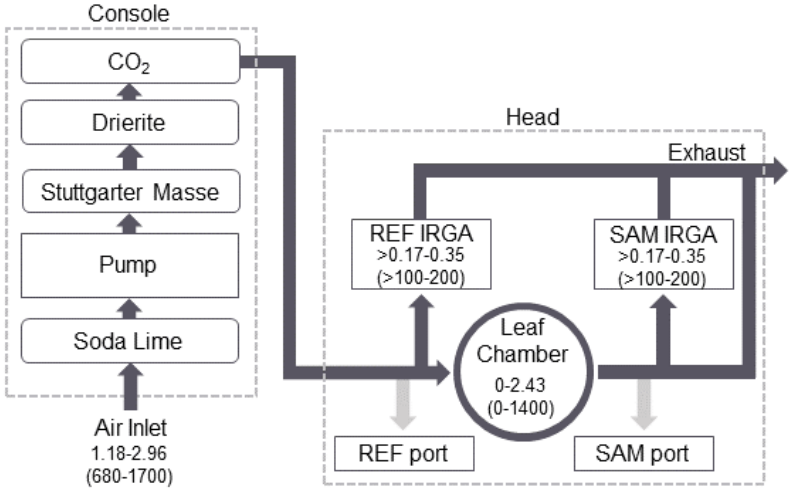

Figure 1. Flow chart diagram of air flow through the PPS during emissions sampling. Dashed lines delineate flow through the PPS console and the head. Dark grey lines show the flow through the PPS during photosynthesis measurements. Light grey lines indicate the additional flow path during emissions sampling. Values for flow rate are given in L min^{-1}, with µmol s^{-1} in parentheses. The order of the chemical treatment of air is shown for the console.

https://doi.org/10.5194/amt-2020-45
Preprint. Discussion started: 25 March 2020

Atmospheric Measurement Techniques Discussions

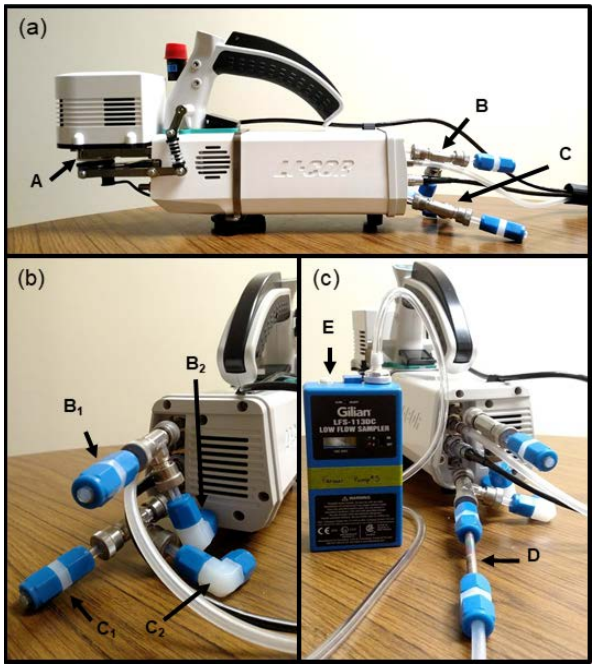

Figure 2. Photograph of the emissions subsampling manifold for the LI-6800. The profile view (a) highlights the leaf chamber (A), SAM subsampling port (B) and REF subsampling port (C). The back view (b), highlights the SAM and REF sampling ports (B_1 and C_1, respectively) and overflow ports (B_2 and C_2, respectively). Panel (c) shows an example setup of sorbent tube (D) emission collection with an external pump (E) sampling the REF subsampling port.

Table 2. Summary of monoterpenes quantified using TD GC/MS.

Compound ($C_{10}H_{16}$)	RT [a] (min)	RSD [b] (%)	LOD [c] (ng)	Emission Rate LOD [d] (ng m^{-2} min^{-1})
α-pinene	3.716 ± 0.008	8.2	0.137	11.4
β-pinene	4.44 ± 0.01	7.4	0.082	6.8
α-terpinene	5.173±0.008	4.5	0.071	5.9
p-cymene	5.354±0.009	5.6	0.111	9.2
d-limonene	5.47±0.01	3.5	0.054	4.5
γ-terpinene	6.306±0.009	2.4	0.085	7.1
terpinolene	7.35±0.01	2.6	0.050	4.2

[a] Retention time
[b] Relative standard deviation (n=10)
[c] Limit of detection, calculated using the propagation of errors approach (Bernal, 2014)
[d] Based on a 20 min sampling time

https://doi.org/10.5194/amt-2020-45
Preprint. Discussion started: 25 March 2020

Atmospheric Measurement Techniques Discussions

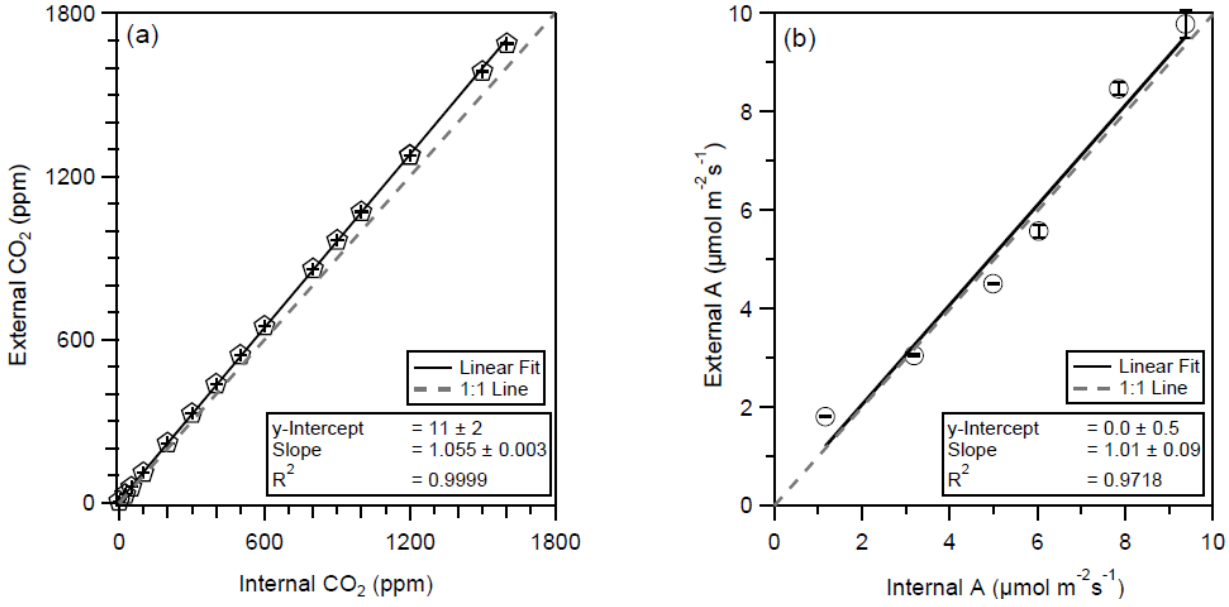

Figure 3. Correlation plots of CO_2 concentration (squares, left panel) and CO_2 assimilation (A, circles, right panel) as calculated internally by the PPS (x-axis) and externally by the CO_2 analyzer (y-axis). A 1:1 line is present as a grey, dashed line. Linear regression fit is shown with a solid line, and fit parameters accompany in text, ± standard error of the fit. Error bars represent the standard deviation of values.

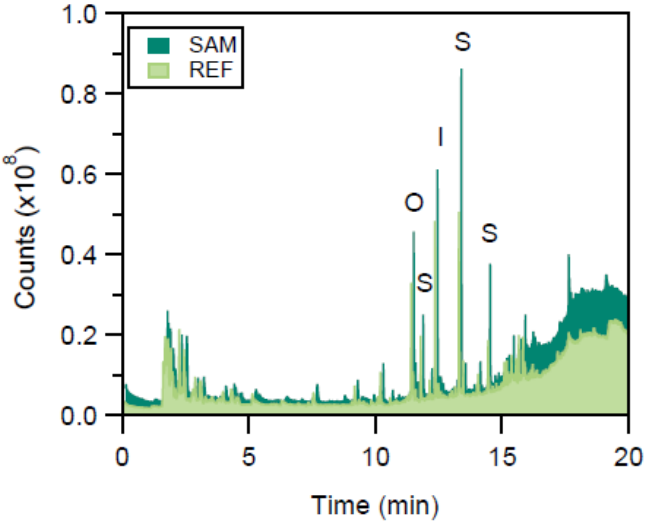

Figure 4. Stacked chromatograms of the background composition of the LI-6800, comparing measurements taken from the REF (light green) and SAM (dark green) ports as sampled by TD-GC-MS (20 minutes at 0.2 L min^{-1}, sampled on Tenax cartridges). The five largest peaks are labeled: S is the result of a siloxane, I is that of isobornyl acrylate and O is of n-octyl acrylate.

https://doi.org/10.5194/amt-2020-45
Preprint. Discussion started: 25 March 2020

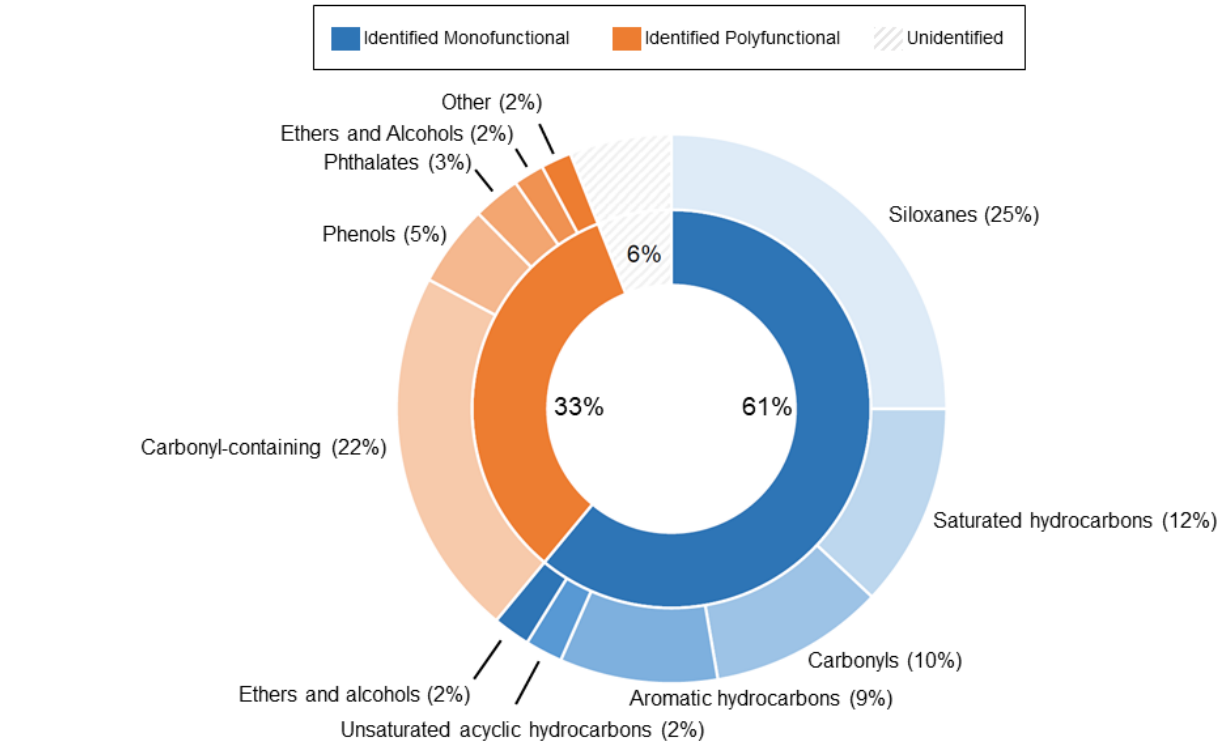

Figure 5. Pie chart summarizing the background composition of the LI-6800 with no leaf in the chamber, collected using the SAM port of the PPS. Percentages are provided to indicate the contribution of each class of compounds to the total integrated peak area. The inner pie chart shows the division of total ion counts for identified monofunctional (containing a single functional group), identified polyfunctional (containing multiple functional groups) and unidentified (yellow stripes) peaks. Identification required an integrated peak area over 50,000 counts and a NIST library match score of at least 500. The outer pie chart shows the subsequent breakdown of both identified classes.

https://doi.org/10.5194/amt-2020-45
Preprint. Discussion started: 25 March 2020

Atmospheric Measurement Techniques Discussions

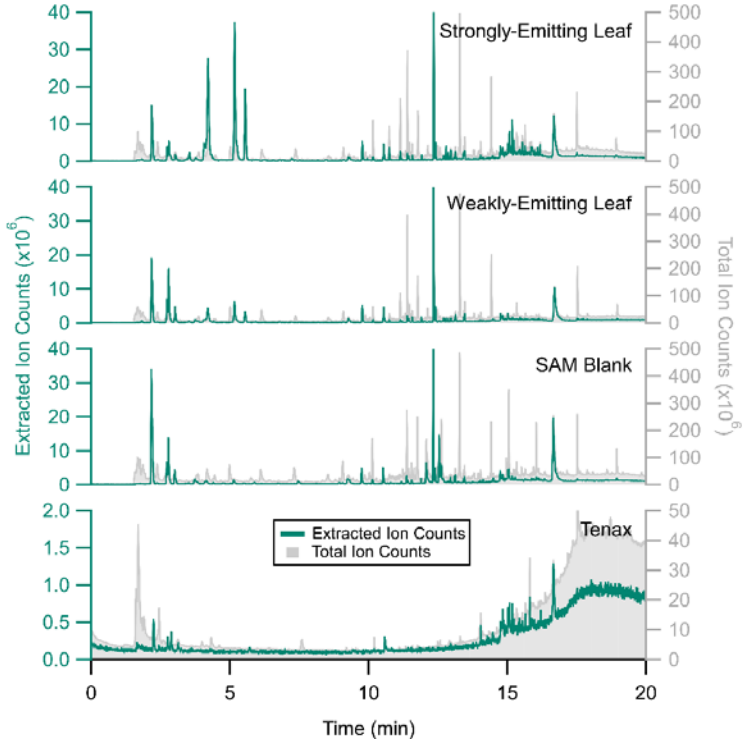

730

Figure 6. Stacked chromatograms comparing extracted ion chromatograms (EIC using *m/z* 136, 135, 93 and 91, left, in green) with the total ion chromatogram (TIC, right, in grey) for a Tenax blank, a SAM blank, a weakly- and a strongly- emitting citrus leaf (*Citrus limon* × *Citrus medica*). Note the difference in axis scales between EIC and TIC. While several background peaks remain in the EIC, there are substantially fewer in the 10+ minute range. Peak height of EIC isobornyl acrylate (RT = 12.3 min) in has been 735 **truncated. Note that retention times differ from Table 2; the column length had been shortened by the time of these measurements.**

https://doi.org/10.5194/amt-2020-45
Preprint. Discussion started: 25 March 2020

Atmospheric Measurement Techniques Discussions

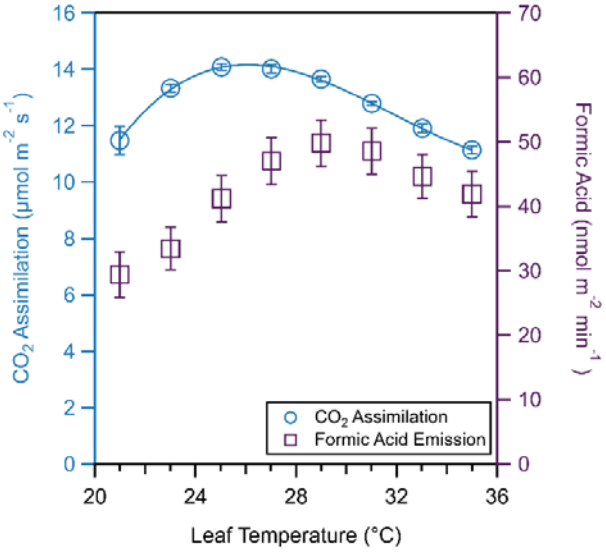

Figure 7. CO_2 assimilation (blue circles) and formic acid emission (purple squares) temperature response curve of one spearmint leaf. Temperatures varied by 2 °C from 21 to 35 °C. CO_2 assimilation follows the expected cubic fit. We collected assimilation and formic acid emission measurements for five minutes and averaged the values of each; error bars represent the standard deviation of those averages.

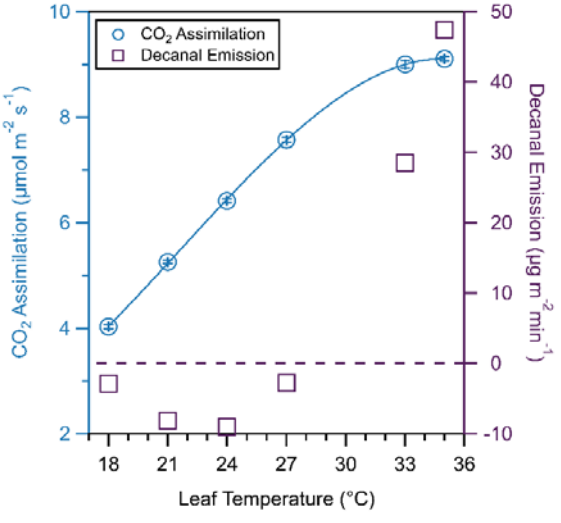

Figure 8. CO_2 assimilation (blue circles) and decanal emission (purple squares) temperature response curve of one basil leaf. CO_2 assimilation is fit to a cubic function. We collected CO_2 assimilation values ten times over 20 minutes and averaged the values; error bars represent the standard deviation of those measurements. We did not collect duplicates of decanal emissions. The dashed line denotes 0 μg m^{-2} min^{-1} decanal emission.

https://doi.org/10.5194/amt-2020-45
Preprint. Discussion started: 25 March 2020

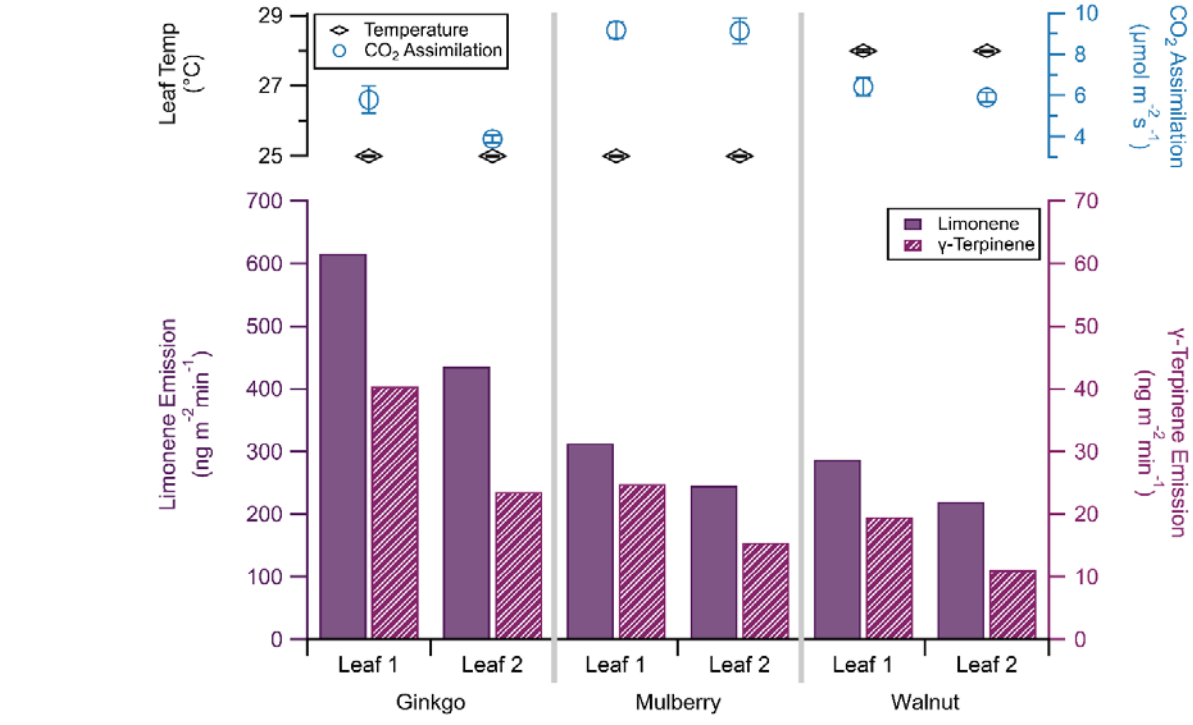

Figure 9. Limonene (solid bars, left bottom axis) and γ-terpinene (striped bars, right bottom axis) emission of two leaves from each of three plant species: ginkgo, mulberry, and walnut. Note that the scale of the limonene emission axis is ten times that of the γ-terpinene emission axis. Leaf temperature (black diamonds, left top axis) and CO_2 assimilation (blue circles, right top axis) are included, with standard deviation bars (n = 60).

https://doi.org/10.5194/amt-2020-45
Preprint. Discussion started: 25 March 2020


Atmospheric Measurement Techniques Discussions

765 **Acknowledgements**

We thank Dr. Karolien Denef for assistance with the GC/MS in the Central Instrument Facility CORE at Colorado State University and Elizabeth Gordon (Li-Cor, Inc.). We thank James Mattila for his assistance with CIMS calculations, and Tyson Berg and Jarod Snook for his assistance with data collection.

Data Availability

770 Data presented in figures herein may be accessed online at https://osf.io/8cs75/?view_only=9fddf94a16e94fd2a50289e01717ec65.

Author Contribution

MR, DL, and DF designed the experiments and MR and DL carried them out. MR analysed the data in consultation with DL and DR. MR and DF prepared the manuscript.

775 **Competing Interests**

The authors declare that they have no conflict of interest.